A Novel Biometallic Interface: High Affinity Tip-Associated Binding by Pilin-Derived Protein Nanotubes

Bin Yu[1], Carmen L. Giltner[2, †], Erin J. van Schaik[2, ‡], Daisy L. Bautista[2], Robert S. Hodges[3], Gerald F. Audette[4], D. Y. Li[1, 5], and Randall T. Irvin[2, *]

[1]*Department of Biomedical Engineering, University of Alberta, Edmonton, AB, Canada*
[2]*Department of Medical Microbiology and Immunology, 1-21 Medical Sciences Building,*
University of Alberta, Edmonton, AB, T6G 2H7, Canada
[3]*Department of Biochemistry and Molecular Genetics, University of Colorado Health Sciences*
Center at Fitzsimmons, RC1 South Tower, Rm. 9121, Aurora, CO 80045, USA
[4]*Department of Chemistry, 456 Chemistry Building, York University, Toronto, ON, M3J 1P3, Canada*
[5]*Department of Chemical and Materials Engineering, University of Alberta, Edmonton, AB, Canada*

The type IV pili of *Pseudomonas aeruginosa* are essentially protein nanofibres composed of multiple copies of a single pilin subunit. Type IV pili extend from the bacterial surface, and mediate specific adherence to biotic and abiotic surfaces. While deletion of the N-terminal region of the pilin's α-helix allows for the ready expression of a highly soluble monomeric pilin protein, incubation of the monomeric protein with undecanethiol results in pilin oligomerization into protein nanotubes. In the present study, the ability of pilin-derived protein nanotubes to bind to grade 304 stainless steel surfaces was evaluated. Protein nanotubes bound to stainless steel with high affinity. Protein nanotube surface binding was observed to be a tip-associated event through competitive inhibition with a synthetic peptide corresponding to the pilin's C-terminal receptor binding domain. AFM studies established that the protein nanotubes utilize the pilin receptor binding domain to directly interact with the steel surface, demonstrating a 2-fold higher adhesive force for grain boundaries than for regions within grains. The adhesive force of the pilin receptor binding domain with the steel surface was determined by two methods and was conservatively estimated to be in the order of 26–55 pN/molecular interaction. Direct, specific binding of protein nanotubes, and/or receptor binding domain composite materials to a steel surface generates a novel metallo-biomolecular interface that forms preferentially on grain boundaries, enhancing the potential for these unique nanostructures in the development of biologically amenable nanosystems.

Keywords: Protein Nanotubes, Type IV Pili, Pilin, Nanomaterials.

1. INTRODUCTION

The development of novel nanotube solubilization strategies has allowed for modification and creation of functional carbon nanotubes (CNTs);[1, 2] this solubilization of CNTs has led to wide implications for their use in nanotechnological applications.[3–5] Their potential to act as biomolecular probes[4] and function in nanoelectronics,[3]

makes CNTs a fascinating model system for both industrial and medical applications. Indeed, CNTs have been shown to increase neuronal signal transfer, dendrite elongation, and cellular adhesion, demonstrating the functionality of these nanofibres in disease alleviation.[6] Furthermore, magnetic particles have been demonstrated to insert into CNTs to create a magnetic and easily manipulated nanostructure.[7] This suggests that CNTs could be used in nanoelectronic applications including magnetically guided medical devices for drug delivery, as well as wearable electronics.[7–9] However, the fabrications of biological-metal interfaces has proven challenging without employing self-assembled monolayers on gold surfaces. The development a simple, versatile, high affinity

---
*Author to whom correspondence should be addressed.

†Department of Biochemistry, HSC Rm. 4H13, 1200 Main Street West, McMaster University, Hamilton, ON, L8N 3Z5, Canada.

‡Department of Microbiology and Infectious Diseases, HSC B871, University of Calgary, 3330 Hospital Drive NW, Calgary, AB, T2N 4N1, Canada.

biometallic interface could facilitate nanoelectronic and nanomechanical fabrication.

Despite the unique physical and electrochemical properties of CNTs, their use in biological systems remains limited due to toxicity issues, and has received considerable adverse reaction and concern in the general population. CNTs have been demonstrated to lead to cell death through direct cytotoxicity,[10, 11] and through the induction of apoptotic cascades.[12] Methods of increasing the biological application of CNTs have focused on the covalent and non-covalent attachment of biochemical moieties onto a CNT scaffold. For example, the adherence of a carbohydrate mimetic polymer onto a CNT scaffold resulted in CNT-cellular interactions mediated by carbohydrate receptors on the cell surface.[13] Such chimeric molecules provide an intriguing blend of chemical and biochemical properties, and may well lead to novel biotic-CNT interfaces and applications.

Efforts to develop more biologically amenable nanostructures have begun examining the assembly of nanosystems from protein precursors. For example, recent reports on template-driven nanotube assembly has been reported for proteins including human serum albumin[14] and glucose oxidase.[15] These studies demonstrate the feasibility of generating nanotubes from proteins not normally thought to assemble into such structures. Also, Patolsky and colleagues have reported the synthesis of gold nanowires based upon the assembly of gold derivatized G-actin monomers into actin filaments.[16] In our investigations into protein-based nanosystems, we recently reported the non-template driven self-assembly of a biologically-based protein nanotube (PNT; Fig. 1) generated from an engineered form of the PilA protein (pilin).[17] The PilA protein is a 13–15 kDa monomeric protein which normally assembles into the type IV pilus (T4P) in the bacterial pathogen *Pseudomonas aeruginosa*. Native T4P, which mediate bacterial attachment to various surfaces and substrates,[18–20] are long filamentous polar appendages that extend from the bacterium, are 6 nm wide and up to several micrometers long.[21] The PilA binding domain, which mediates binding to both biotic and abiotic surfaces, is encoded within residues 128-144; synthetic peptides that encompass this region have been shown to bind biotic and abiotic surfaces.[20] *P. aeruginosa* colonization of stainless steel surfaces is of interest both medically and industrially. In clinical settings, stainless steel and instrument colonization generates a significant reservoirs of the pathogen, resulting in elevated noscomial infection rates, as well as increased morbidity and mortality. Industrially, *P. aeruginosa* biofilm formation is associated with corrosion issues and product contamination. The molecular basis for T4P mediated binding to steel surfaces, while of considerable interest, has not been extensively investigated. PNTs, generated from a truncated form of the pilin protein, have been shown to be structurally similar to T4P,[17] and are an ideal
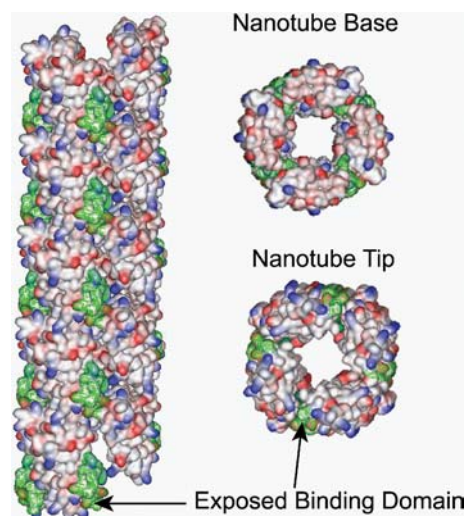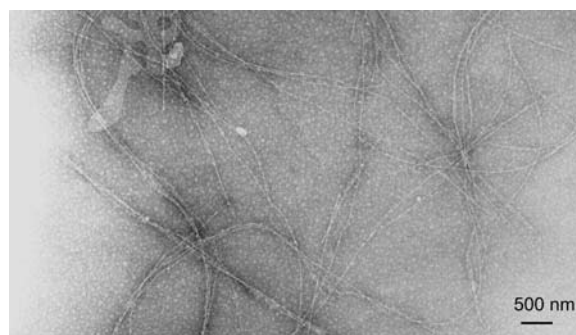
Fig. 1. Pilin-derived protein nanotubes (PNTs). (a) Transmission electron micrograph of K122-4 pilin PNTs negatively stained with 1% uranyl acetate as imaged in a Philips EM301 electron microscope operating at 80 kV. (b) Molecular model of PNTs employing a 3-start left-handed helical fiber structure of type IVa pilins proposed by Craig et al.[38] The pilin receptor binding domain for stainless steel is colored green, while red and blue coloring indicates acidic and basic electrostatic potential, respectively, and white represents hydrophobic surfaces.

candidate for the development of a biologically amenable nanostructure for bionanotechnological applications.[22]

In the current report, we demonstrate that PNTs retain biological functionality and can bind with high affinity to stainless steel surfaces. We report that PNT binding to a stainless steel surface is similar to that observed for native T4P, and appears to involve a trivalent interaction with the metal surface. PNT interaction with the steel surface is mediated through a small receptor binding domain that interacts directly with the steel surface, preferentially at grain boundaries (GBs). We estimate, utilizing atomic force microscopy (AFM), that the attractive or adhesive force between a receptor binding domain and the steel is in the range of 26–55 pN/molecular interaction, and PNT-stainless steel adhesive force is in the range of 78–165 pN/PNT-steel interface. The binding of PNTs to stainless steel generates a novel metallo-biomolecular interface, furthering the potential of these unique nanostructures for use in bionanotechnology.

2. MATERIALS AND METHODS

2.1. Purification of Pili, Monomer, and Protein Nanotubes

K122-4 pili were purified from *P. aeruginosa* as previously described.[23] Monomeric truncated K122-4 pilin was purified from *E. coli* cells harboring plasmids containing *P. aeruginosa* strain K122-4 PilA(Δ1-28).[24, 25] K122-4 pilin-derived PNT formation was preformed as outlined by Audette and colleagues,[17] where 1.1 M undecanethiol in methanol containing DTT and EDTA was added to pilin monomers, triggering nanotube oligomerization.

2.2. Synthetic and Recombinant Peptide Synthesis

All synthetic peptides used in this study were synthesized by solid phase as previously described.[20] All peptides are N-α-acetylated with a free carboxyl. Peptides with a formed disulfide bridge between cysteine 129 and 142 are identified by an ox. E-coil PAK(128-144)ox was expressed recombinantly from a pRLD-E plasmid where the PAK(128-144)ox DNA sequence was spliced in-frame with the E-coil utilizing synthetic oligonucleotides and expressed in *E. coli* strain BL-21 as previously described.[20] The expressed peptide was purified by metal affinity chromatography, the purity and formation of the disulfide bridge was confirmed by mass-spectroscopy and N-terminal protein sequencing. The sequences of the peptides used in this study are shown in Table I.

2.3. Stainless Steel Binding and Competitive Inhibition Assays

Grade 304 stainless steel 2B finish coupons were prepared as outlined in Giltner et al.[20] Purified monomeric pilin or PNTs (100 μl/well) were added in replicates of six to the steel manifold and incubated with gentle agitation for one hour at 37 °C. Steel coupons were washed five times with Buffer A (PBS pH 7.4 with 0.05% BSA), and binding was assessed using a polyclonal anti-K122-4 antibody followed by secondary goat-anti-rabbit HRP (BioRad). Substrate buffer (0.01 M sodium citrate buffer pH 4.2 containing 1 mM 2,2'-Azino-bis-(3-ethylbenzthiazoline-6-sulfonic acid) diammonium salt (ABTS; Sigma) and 0.03% (v/v) hydrogen peroxide) was added to steel manifolds as described.[20] Absorbance (405 nm) was measured

after a 10 minute incubation with substrate buffer and using a Multiscan Plus version 2.01 plate reader.

For competitive inhibition assays, monomeric pilin and PNTs (0.75 μg/ml) were mixed with PAK(128-144)ox in PBS pH 7.4 so that the final peptide concentration ranged from 0.512 pM to 5.12 nM. Samples were then assayed for stainless steel binding as described above.

2.4. Preparation of Peptide Derivatized AFM Tip for Adhesive Force Measurement

Surface adhesive force that occur between two surfaces can be measured using an atomic force microscope (AFM).[26, 27] An AFM (Digital Instruments) employing the "contact mode" was used to determine the adhesive force between the AFM tip and a target surface. Figure 2 schematically illustrates the deflection of a cantilever (connected with an AFM tip) as a function of displacement when approaching and leaving a sample surface under external driving force. When the AFM tip is eventually pulled away from the surface, the tip does not leave immediately due to the adhesive force between the sample surface and the AFM tip, which results in deflection of the cantilever (line 5–6 in Fig. 2). The deformation of the cantilever corresponding to this deflection reflects the adhesive force. The deflection of the cantilever is detected by a laser beam, from which the related force can be quantitatively determined if the spring constant of the cantilever is known. Figure 2 illustrates how the cantilever is deflected during the entire AFM tip approaching and leaving process. The spring constant of the cantilever in the current AFM study is 0.06 N/m.

In this study, a PAK(128-144)ox peptide-coated AFM tip was used to measure the adhesive force between the tip and a steel surface. As the synthetic receptor binding domain is small (roughly rectangular in nature with dimensions of ∼15.7 Å by ∼17.5 Å), coupling the peptide directly to the AFM tip could compromise the interaction of the peptide with a steel surface area on a nano/micro scale. An approach was utilized to indirectly derivatize AFM tips with the peptide being presented on a coiled-coil structure such that the peptide would be maintained ∼41 Å way from the AFM tip surface allowing the receptor binding domain more freedom to interact with the metal surface. A *de novo* designed heterodimeric coiled-coil system was utilized for this application,[28, 29] which

Table I. Synthetic peptides and peptide sequences employed or referred to in this study.

Peptide	Sequence
PAK(128-144)ox	Ac-K-**C**-T-S-D-Q-D-E-Q-F-I-P-K-G-**C**-S-K-OH
PAO(128-144)ox_Scrambled	Ac-N-**C**-P-D-F-D-P-T-K-K-G-M-Q-A-**C**-T-S-OH
PAO(128-144)ox	Ac-A-**C**-K-S-T-Q-D-P-M-F-T-P-K-G-**C**-D-N-OH
Cys-K coil	Ac-C-(K-V-S-A-L-K-E)$_5$-OH
E-coil	Ac-(E-V-S-A-L-E-K)$_5$-OH
E-coil PAK(128-144)ox	H$_5$-(E-V-S-A-L-E-K)$_5$-K-**C**-T-S-D-Q-D-E-Q-F-I-P-K-G-**C**-S-K
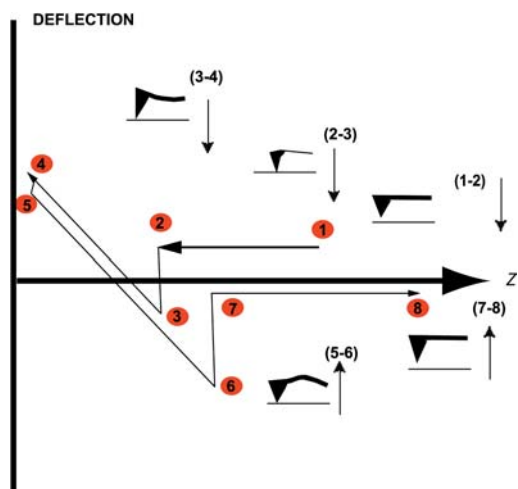
Fig. 2. AFM method of determining adhesive force measurements. The curve of deflection versus displacement (Z) of cantilever when the AFM tip is approaching and leaving a sample surface. A recorded deflection versus Z curve is also presented in the same figure. 1–2: The AFM tip is pushed by the cantilever towards a sample surface; 2–3: The tip is pulled down by an attractive force from the sample surface; 3–4: The cantilever is bent up as the tip touches the surface under an applied force; 5–6: The tip is attracted by the adhesive force when pulled away from the sample surface; 6–7: The tip escapes from the surface when the external force exceeds the adhesive force, which can be determined if the spring constant of cantilever is known; 7–8: The tip moves away from the sample surface.

consists of a 35 residue K-coil which is coupled to the AFM tip and serves to capture a 35 residue E-coil[30] with the receptor binding domain (PAK(128-144)ox) fused to the C-terminus of the E-coil peptide. The affinity of the coiled-coil interaction is 60 pM[31] and the resulting coiled-coil is an extraordinarily stable structure that is only partially dissociated in solvent at a temperature of 80 °C.[32] The derivatization process is illustrated in Figure 3. A standard AFM silicon nitride tip was coated with 20 nm of Au by sputter coating, and then immersed in 25 μM K-coil peptide synthesized with an additional N-terminal cysteine residue in PBS pH 7.2 for 40 min at room temperature such that the K-coil was coupled to the Au coating through the free sulfhydryl of the cysteine residue. The derivatized AFM tip was then washed with distilled H_2O and then immersed in 5 mM cysteine in PBS pH 7.2 for 40 minutes at room temperature, washed with distilled H_2O and then immersed in 1 μg/ml of E-coil-PAK(128-144)ox for 40 minutes at room temperature to allow the formation of the heterodimeric coiled-coil with the receptor binding domain being displayed on the end of the E-coil at the tip of the AFM tip. Alternatively, synthetic E-coil was utilized to generate an Au-coated AFM tip which displayed only the heterodimeric coiled-coil construct as a control AFM tip. The functionalized tips were then washed with distilled H_2O and then air dried for subsequent use. The peptides were prepared as previously described with the purity of the peptides being confirmed by HPLC reversed phase chromatography and mass
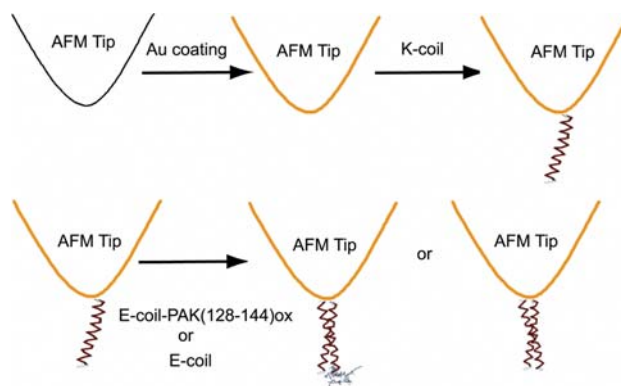

Fig. 3. Schematic diagram of the derivatization of a standard AFM tip with a coiled-coil displayed PAK(128-144)ox pilin receptor binding domain. As a control, AFM tips were also derivatized with the same coiled-coil where the PAK(128-144)ox sequence was not fused to the E-coil. Sequences of the peptides utilized in this process are presented in Table I.
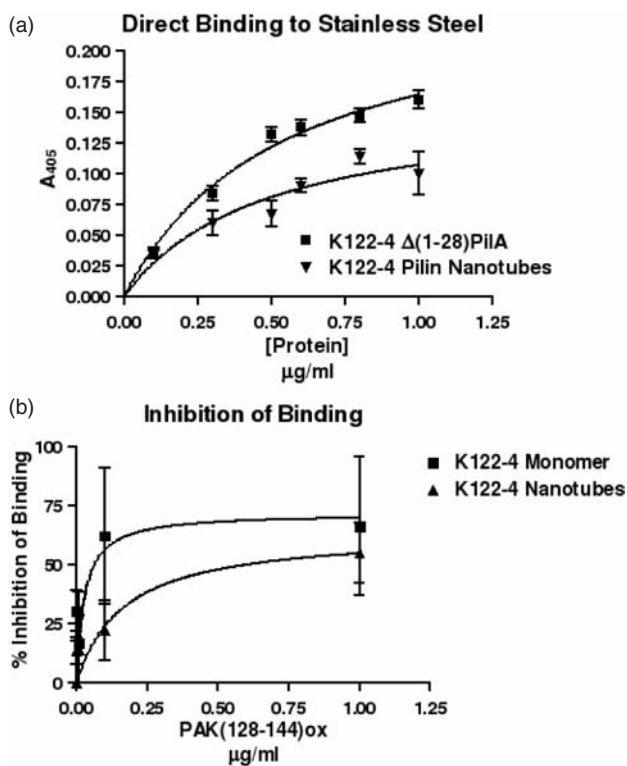
spectroscopy.[20] Additional peptides utilized in this study include a synthetic PAO pilin receptor binding domain (PAO(128-144)ox) and the scrambled PAO pilin receptor binding domain (PAO(128-144)ox_Scrambled). The purity of these peptides, and the oxidation state of the disulfide bond was confirmed as previously described,[20] and Table I describes all peptide sequences used in this study.

2.5. Characterization of Steel Surfaces and AFM Adhesive Force Determination

Commercial grade 304 stainless steel specimens with dimensions of $2 \times 2 \times 2$ cm were annealed at 1160 °C for 20 minutes in Ar atmosphere followed by air cooling. The steel surface was smoothed by the use of sand papers up to 1200#, and then polished with an aqueous slurry of 0.05 μm colloidal silica. The polished sample surface was etched with a hydrochloride/nitric acid solution for 10 sec, washed ultrasonically with reagent grade acetone (10 min),
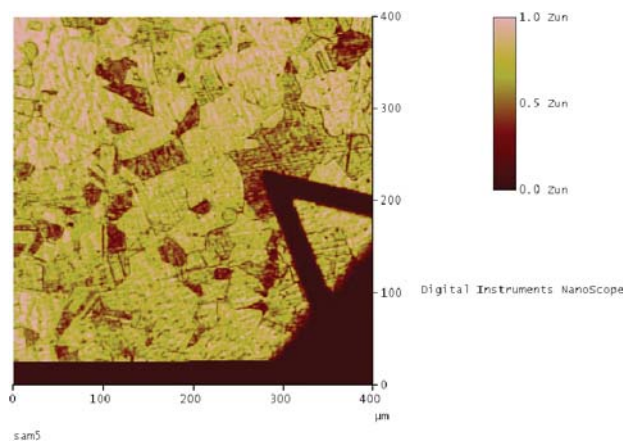

Fig. 4. An optical image of a grade 304 stainless steel surface used in this study obtained in polarized light with the AFM. Note the obvious grains, grain boundaries, and the AFM probe.

(a)

Direct Binding to Stainless Steel

- ■ K122-4 Δ(1-28)PilA
- ▼ K122-4 Pilin Nanotubes

(b)

Inhibition of Binding

- ■ K122-4 Monomer
- ▲ K122-4 Nanotubes

Fig. 5. Monomeric pilin and PNT binding to stainless steel surfaces. (a) Direct binding of K122-4 Δ(1-28)PilA monomer (■) and K122-4 PNTs (▼) to grade 304 stainless steel surfaces as a function of protein concentration. (b) Competitive inhibition of K122-4 Δ(1-28)PilA monomer (■) and K122-4 PNTs (▲) binding to steel by PAK(128-144)ox.

95% ethanol (5 min), rinsed with H_2O (deionized, then filtered to remove ions, organics and particles immediately before use), and air dried. The average grain size of the stainless steel specimens was ∼30 μm, as determined by microscopic examination employing polarized light.
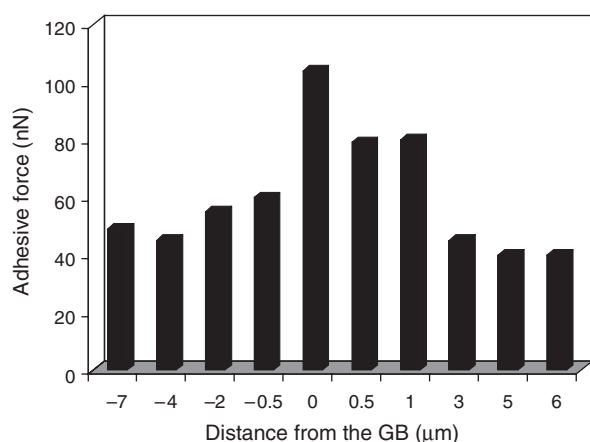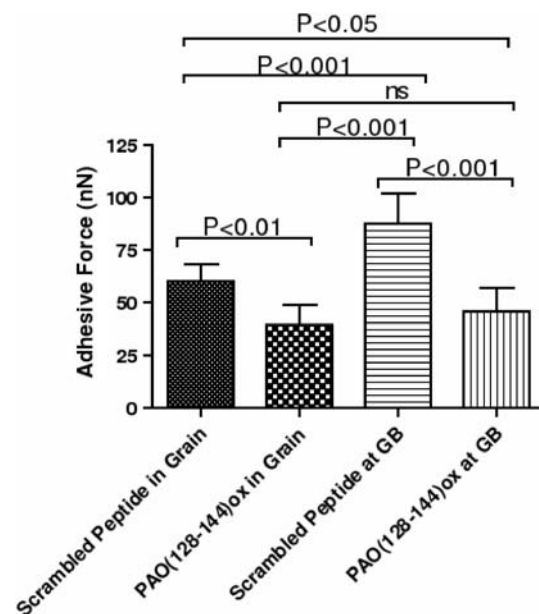

Fig. 6. Adhesive force measurements of a PAK(128-144)ox derivatized AFM tip with stainless steel as a function of distance from the GB. Measurements are for a single experiment with the profile across a single GB. These measurements demonstrate the considerable increase in observed adhesive force for the peptide-derivatized AFM tip over that of a standard Si_3N_4 AFM tip (30.5 ± 1.0 nN) at and near GBs.
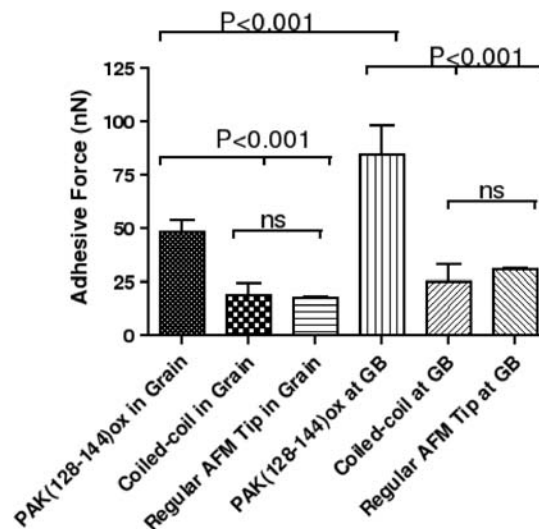
Fig. 7. Adhesive force measurements of AFM tips derivatized with coiled-coils fused with PAK(128-144)ox and AFM tips derivatized with coiled-coils which lacked the PAK(128-144)ox sequence with stainless steel within and at GBs. A one-way ANOVA analysis of the adhesive force measures was utilized to determine the probabilities of the data being significantly different.

In order to determine the adhesive force between steel surfaces and the pilin receptor binding domain, the adhesive force between the AFM tip and a stainless steel surface was measured by two experimental approaches: (1) a direct measurement employing a coiled-coil derivatized tip as a reference, and (2) abolishing the interaction by pre-treating the surface with a synthetic receptor

Fig. 8. Adhesive force measurements of AFM tip derivatized with peptide and stainless steel that had been pre-treated with either PAO(128-144)ox peptide to inhibit PAK(128-144)ox binding to the steel or with PAO(128-144)ox_Scrambled peptide which does not interact with the steel surface.

binding domain or a scrambled receptor binding domain sequence that does not interact with steel (PAO(128-144)ox_Scrambled) as a control. The AFM tip was moved from one grain to another utilizing the optical controls of the AFM (Fig. 4) so that the adhesive force at different grains and GBs could be determined.

2.6. Statistical Analyses

Statistical analyses of all assays were preformed with GraphPad Prism Version 4.0. *P*-values were determined to be significant at $P < 0.05$. A non-parametric one-way ANOVA test of the data (the observed data did not differ significantly from normally distributed data, but some portions of the data were significantly skewed) was employed to determine the statistical significance of the results. Individual binding assays, with six replicates per assay, were repeated in triplicate. Error bars in Figure 5 represent ±SEM, while for Figures 7 and 8 represent ±SD.

3. RESULTS

3.1. Adherence to Biotic and Abiotic Surfaces

The structure of the K122-4 pilin monomer is composed of an N-terminal α-helix packed onto a four-stranded antiparallel β-sheet, connected by a highly variable loop region, and a C-terminal disulfide bonded receptor binding domain (D-Region).[25, 33–36] However, the first 28 N-terminal residues of the α-helix (α1-N), which are exposed from the rest of the protein, are highly hydrophobic. The hydrophobic α1-N region has been proposed to serve as an oligomerization domain for native type IV pilus assembly,[37, 38] a process achieved through the effects of over 50 separate proteins in the bacterium.[39] Truncation of the α1-N domain yields a highly soluble monomeric pilin[24, 25, 34, 35] which is unable to form a native pilus structure. Rather, upon exposure to a hydrophobe, the highly soluble truncated pilin monomer oligomerizes into long, thin nanotubes (PNTs; Fig. 1(a)).[17] PNTs, which like native pili are made up of thousands of pilin monomers,[36, 38, 40, 41] can reach lengths upwards of 100 μm, considerably longer than native T4P.[17, 21] As it is known that native T4P mediate bacterial adherence to a variety of biotic[36, 42–44] and abiotic[20, 45] surfaces, in particular binding with high affinity to stainless steel surfaces, we investigated the possibility that pilin-derived PNTs may function in a similar fashion.

As T4P and the PilA receptor binding domain have been shown previously to bind with high affinity to stainless steel surfaces,[20] the ability of monomeric pilin, and PNTs to bind to Grade 304 stainless steel was assessed. Pilin-derived PNTs were observed to bind Grade 304 stainless steel in a concentration dependent and saturable manner (Fig. 5(a)). The concentration dependent binding by monomeric pilin (Fig. 5(a)) occurs as the receptor binding domain is completely surface exposed. It should be noted

that the binding curves for the monomer and PNTs are not directly comparable as each PNT molecule is composed of thousands of monomers.

3.2. Competitive Inhibition of Surface Adherence

T4P surface adhesion is mediated through the C-terminal receptor binding domain (D-region) of the pilin monomer.[42, 43] Current assembly models of type IV pili,[33–36] and by extension pilin-derived PNTs,[17, 22] result in a limited number of non-occluded receptor binding domains being available for surface adherence being displayed at the tip of the structure. To determine whether functional receptor binding domains in PNTs are indeed limited, competitive peptide inhibition studies were preformed using the synthetic peptide PAK(128-144)ox, a well characterized synthetic receptor binding domain.[46] The PAK(128-144)ox peptide corresponds to the D-region of the PilA protein (residues 128-144), is oxidized to form an internal disulfide bond, and has previously been demonstrated to specifically inhibit *P. aeruginosa* strain K122-4 binding to stainless steel.[20] The PAK(128-144)ox peptide was observed to competitively inhibit K122-4 monomer and PNT adhesion to stainless steel surfaces (Fig. 5(b)). Peptide inhibition was greater for the monomer than for PNTs (Fig. 5(b)). PNT binding to steel surfaces demonstrates a higher ($\sim$10 fold) apparent affinity (or more accurately avidity) for the steel surface (given the larger amounts of peptide required to inhibit binding to an equivalent level) compared to the monomer. The difference in the apparent affinities for steel indicates that >1 receptor binding domain mediates contact of the PNT with the steel surface. However, the vast majority of receptor binding domains in each PNT molecule must be occluded in the PNT due to monomer packing constraints as inhibition of binding was readily observed. The data is consistent with each PNT tip presenting 3 functional receptor binding domains that mediate binding to the steel surface.

3.3. Direct Interaction of the Receptor Binding Domain with Steel

The high affinity interaction of the receptor binding domain with the steel surface has not yet been well characterized, nor has the possibility that the interaction with the steel surface occurs indirectly through the interaction of the receptor binding domain with an absorbed conditioning film rather than the steel surface directly. To investigate this potential, a direct force measurement approach (also termed force mapping) utilizing AFM in a "dry" (normal building relative humidity, 30–40% RH) air environment with polished and etched steel was utilized. The polishing and etching process removes surface conditioning films and surface adsorption of organics from air onto steel is not problematic. Employing a "dry" surface minimizes the bulk solvent hydrophobic interactions. While the peptides

will retain bound or solvated water molecules, the lack of bulk solvent ensures that any adhesive force measurements reflect the forces generated by the interaction of the peptide with the metal surface rather than interaction forces generated by hydrophobic effects, largely generated by bulk solvent energetic contributions.[47, 48]

3.4. Adhesive Force at Grain Boundaries and Within Grains

The adhesive force of standard Si_3N_4 AFM tip within the central region of metal grains is relatively low and, as anticipated (due to the altered physical–chemical properties of GBs), near and at GBs the adhesive force was observed to increase significantly. In this study, the adhesive force was determined with 20 grains and their associated GBs (replicated 3 times). The average adhesive force within a grain and at the GB was significantly different ($P < 0.001$), with the adhesive force being 17.5 ± 1.0 nN within the grain and at a GB the adhesive force was 30.5 ± 1.0 nN. The results indicate that the adhesive force at GB was ∼1.74 fold higher than that observed within grains. The increased adhesive force at GBs is largely attributed to an increase in electron activity at a GB; this interpretation has been confirmed by measuring decreased electron work function (EWF) at GBs in other metals.[49–52] Bacterial adherence and biofilm formation occurs preferentially at GBs,[20, 45] and such is the case with *P. aeruginosa* pilus mediated binding to steel.[20] Employing a receptor binding domain derivatized AFM tip revealed that the adhesive force was considerably higher than that observed with the standard Si_3N_4 AFM tip, and the adhesive force also increased significantly at and near GBs (Fig. 6).

### 3.5. Adhesive Force of Receptor Binding Domain Derivatized Tips and Steel

The adhesive force between the derivatized AFM tip and the stainless steel surface was then determined as described above (20 GBs and their respective grains were examined with each observation being replicated 3 times). The mean adhesive force at the GB for the peptide derivatized tip was 86.8 ± 13.3 nN while the mean adhesive force within a grain was observed to be 47.6 ± 10.7 nN (Fig. 7). This represents an increase of 2.84 fold and 2.72 fold in the adhesive force between the derivatized AFM tip relative to the standard AFM tip for the GB and within the grain, respectively, with the GB adhesive force being ∼1.82 fold greater than that observed within the grains. The derivatized AFM tips were robust and did not exhibit any evidence of performance decay or change until ∼80 independent measurements were taken. While these observations provide evidence that the receptor binding domain mediates direct binding to the steel surface, the derivatized AFM tip varies considerably from the standard AFM tip (i.e., 20 nm Au

coating, and multiple coiled-coil constructs with displayed receptor binding domains).

To ascertain how much of the additional adhesive force was attributable to the receptor binding domain-steel interaction two independent strategies were utilized. First, the adhesive force of control derivatized AFM tips were determined by employing AFM tips coated with Au and derivatized with an equivalent concentration of the heterodimeric coiled-coil, but where there was no receptor binding domain present. Second, the steel surface was pre-treated with either a synthetic receptor binding domain previously demonstrated to inhibit pilus mediated binding to steel (PAO(128-144)ox), or a peptide that had the same amino acid composition as the receptor binding domain but where the amino acid sequence was altered such that the peptide did not bind to steel (PAO(128-144)ox_Scrambled).[20] Following this surface pre-treatment, the adhesive force of a derivatized AFM tip that displayed a receptor binding domain on the coiled-coil structures was measured. The additional approach utilizing a scrambled non-functional peptide sequence displayed on the coiled-coil structures was not deemed feasible. This was due to significant difficulties in oxidizing the two cysteine residues in the scrambled sequence to form the disulfide bond found in the native receptor binding domain (extremely low yields of the PAO(128-144)ox_Scrambled peptide were obtained in multiple syntheses), resulting in a high probability of free sulfhydryl groups that would confound our studies given the Au coating of the AFM tip.

Adhesive force measurements with coiled-coil derivatized AFM tips indicate that the derivatization of the AFM tip had minimal effect on the adhesive force measurements relative to the standard AFM tip (Fig. 7). The adhesive force attributable to the PAK(128-144)ox receptor binding domain interaction with the steel surface can therefore be deduced to be 28.0 ± 11.3 nN within grains and to be 62.2 ± 14.5 nN, a significant ($P < 0.001$) 2.22 fold difference (Fig. 7).

An alternative approach for determining the adhesive force attributable to the PAK(128-144)ox peptide-steel interaction is to pre-treat the steel surface with saturating concentrations of a synthetic peptide that binds to the steel surface, thereby preventing PAK(128-144)ox binding to the steel. A synthetic receptor binding domain derived from PAO pilin, PAO(128-144)ox, has previously been shown[20] to inhibit interaction with steel (this peptide does not interact with either the PAK(128-144)ox peptide or with the derivatized AFM tip, data not shown). Conversely, the scrambled peptide (PAO(128-144)ox_Scrambled) does not bind to steel and does not prevent PAK(128-144)ox binding to steel.[20] Utilizing this approach, the adhesive force attributable to the PAK(128-144)ox-steel interaction was deduced to be 20.2 ± 12.6 nN within grains and was significantly ($P < 0.001$) higher (2.12 fold) at 43.0 ± 18.3 nN when measured at the GBs (Fig. 8). These results, obtained
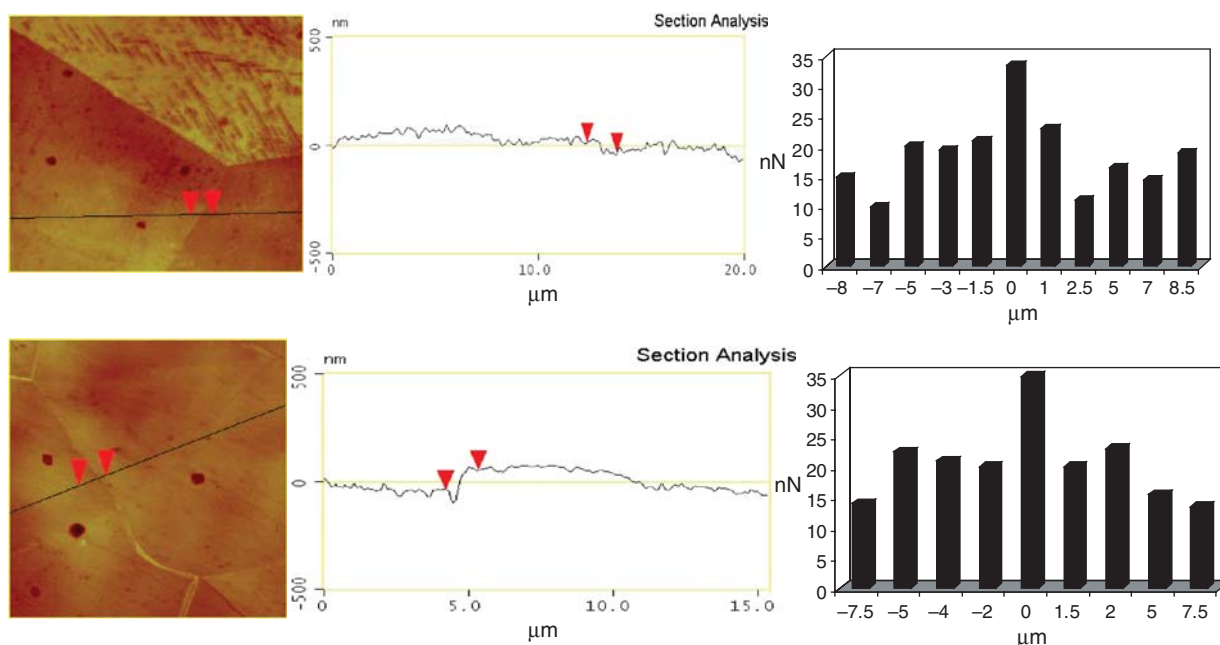
Fig. 9. Adhesive force measurements of a standard Si_3N_4 AFM tip across a GB in steel that had been etched for 10 s (top) and across a GB in steel that had been etched for 20 s (bottom). Note the different AFM surface profiles at the GB, the sample etched for 20 s has greater loss of material at the GB compared to the sample etched for 10 s.

by a competitive approach, are in reasonable agreement with the values previously determined by a direct approach. Notably, both methods report that the peptide-steel interaction is ~2 fold stronger at GBs. Averaging the results obtained by the two experimental approaches, the adhesive force attributable to the peptide-steel interaction indicates that within the grains the force of interaction is 24.1 nN and ~2.2 fold higher (52.6 nN) at GBs.

The observation that the adhesive force between the peptide and the GB was enhanced relative to what could be attributed to the basic material properties of the steel GB raised the question as to the basis for the enhanced interaction of the peptide with the GB. Acid etching of the steel surface causes a loss of material at GBs, and the possibility that the altered geometry of the GB could affect the adhesive force measurements was considered. Steel samples were etched for 10 or 20 seconds, respectively, and the degree of loss of material was determined by AFM examination of GBs using a standard Si_3N_4 AFM tip. We observed no difference in the adhesive force at the GB of steel surfaces etched for the different periods of time, although the geometric difference in the GB was readily determined by AFM (Fig. 9). The differential geometry at the GB on etched surfaces did not contribute to observed differences in the adhesive forces we observed at the GBs.

4. DISCUSSION

4.1. Strength of the Peptide-Steel Interface

One of the biological functions of type IV pili is to power an unusual form of motility. The pilus attaches to solid surfaces through the pilin receptor binding domain and is then retracted or depolymerized back into the cell to effectively pull the cell towards the surface at a rate of 0.5 μm/s with substantial tension on the pilus.[53] In order to determine if our direct force measurements were consistent with the biological observations, we estimated the force required to disrupt a single peptide-steel interaction. The potential number of coiled-coil-PAK(128-144)ox molecules that were displayed on an AFM tip, and which could potentially interact with the surface of a stainless steel specimen was conservatively estimated. The average length of coiled-coil is approximately 82.5 Å, and the tip of a gold-coated AFM tip is roughly a spherical cap with a radius of 70–90 nm (R), bearing in mind that the Au coat is ~20 nm thick. Therefore, the effective potential contact area may be conservatively estimated as being between 513083 Å^2 ($R = 70$ nm) and 1.3×10^6 Å^2 ($R = 90$ nm). The minimal surface area occupied by a vertically attached coiled-coil is represented by a rectangle (as determined by an examination of molecular structures of a number of two stranded anti-parallel coiled-coils available in the PDB) of 26 Å $\times$ 21 Å, including a van der waals surface for the molecule and a single hydration layer that is physically associated with the peptides and does not dissociate from the peptide when the peptide is air dried. Thus the minimal surface area occupied by a vertical coiled-coil is ~546 Å^2. Therefore, an AFM tip may accommodate from 940 molecules/AFM tip ($R = 70$ nm) to 2,381 molecules/AFM tip ($R = 90$ nm). Employing the average value reported by the two experimental methods we estimate that the strength of the PAK(128-144)ox steel

interaction is in the range from 10 pN/molecular interaction to 26 pN/molecular interaction within the grain and from 22 pN/molecular interaction to 55 pN/molecular interaction at the GB. Current molecular modeling of the *P. aeruginosa* pilus suggests that the structure consists of 3-intertwined filaments that display 3 independent binding domains at the tip of the pilus.[38] Thus 3 pilin receptor binding domains could enable the pilus to withstand 66 to 165 pN of force when bound to steel. The estimated force measurements are consistent with existing biological data which indicates a retracting pilus is under ~10 pN of stress,[53] and that the native pilus breaks when 120 pN force is applied.[54]

4.2. Molecular Basis for Peptide-Steel Interaction

Bacterial biofilm formation on aqueous surfaces and their associated conditioning films has long been recognized,[55, 56] as has the importance of the substrate's surface free energy. However, accurate modeling of bacterial adhesion to surfaces has been challenging due to the complexities of the systems, conditioning films and hydrophobic interactions of cells and surfaces in an aqueous environment.[57–59] The current experimental approach employs conditions where hydrophobic effects are minimized (non-aqueous, "dry" environment with minimal bulk solvent affects on ligand interactions), and the potential involvement of a conditioning film (the steel surfaces were polished, etched and solvent cleaned) has been largely eliminated. Biologically relevant interactions generally occur in aqueous salt environments where all components are fully hydrated. While the affinity of biological interactions varies substantially, in general apparent affinity constants range from nanomolar to millimolar (most physiologically regulated interactions have an affinity constant in the micromolar range) for univalent interactions; multi-valent interactions allow for much higher apparent affinity constants due to avidity. The interaction of proteins and their ligands is generally highly specific and dependent upon a range of specific molecular interactions and spatial complementarity. However, the affinity and stability of the interaction is largely determined by what are termed hydrophobic interactions.[47] In thermodynamic terms, most of the energetic contribution to receptor-ligand interactions arises from the exclusion of bulk solvent (water) from the interaction site as the change in entropy does not positively contribute to the occurrence of the molecular interaction. The energetic contribution of direct molecular interactions does not generally negate the entropic energy term, but rather confers the specificity of the interaction. Tightly bound water or solvation/hydration waters are not freely exchangeable with bulk solvent, do not contribute to receptor-ligand binding energetics, and are readily observed in protein crystallographic studies of protein-ligand complex interfacial regions. Thus the

very high affinity of the pilin receptor binding domain for stainless steel is unusual due to the domain's high flexibility in both the cognate protein[60] and the synthetic peptide,[61] which increases the entropic penalty for the interaction, as well as the rather small potential interaction area of the monomeric peptide with the steel. This suggests that a hydrophobic effect alone does not account for the affinity of the interaction of the peptide with the steel surface or a conditioning film found on that surface. We thus pursued a methodological approach that reduces the potential of interaction of the peptide with a conditioning film, and constrains the hydrophobic effect. The polishing, etching and washing of the stainless steel removed the bulk water, thereby limiting available H_2O to what can experimentally be defined as solvation (bound) water. Receptor binding domain interactions determined by force mapping represents a system where there is minimal potential for a "conditioning film," with no bulk water to drive or stabilize a molecular interaction between the receptor binding domain and the steel surface. The direct interaction of the peptide with the steel surface was therefore measured by AFM.

A portion of the interfacial interaction between the peptide and steel surface can be directly attributed to material properties of the steel both within grains and at GBs. However, the peptide-steel interaction is dependent on the peptide's sequence rather than it's molecular composition. This interaction displays a significant preference for GBs that exceeds what is predicted based of the difference in surface free energy or material's adhesive force increase at the GB (~2 fold increase for the peptide at the GB as compared to a ~1.7 fold or ~1.3 fold increase observed with standard or coiled-coil derivatized AFM tips, respectively). The pilin receptor binding domain is a self-folding domain that in aqueous solution contains two discrete β-turns[62] and two families of conformers due to the existence of both a *cis* and a *trans* conformation of the proline in the sequence. The solution structure of the PAK pilin receptor binding domain is similar to that observed in the crystal structure of PAK pilin in a low solvent content crystal[34] but the molecular structure of the air dried pilin receptor binding domain is unclear. The molecular basis for the interaction of the peptide and steel is uncertain at this time, but likely results from the stabilization or sharing of surface electrons from the metal in addition to the expected van der Waals interactions. The higher adhesive force at GB could be largely attributed to increased electron activity at GB corresponding to lower EWF.[49] The more active the electrons are at a surface, the more reactive is the surface.[50] Grain boundaries have irregular lattice structures with dislocations and other defects such as voids and vacancies. As demonstrated previously,[51] dislocations can raise electrons' activity and thus render dislocation-containing regions or deformed materials more anodic or reactive.[52] It should be mentioned that high

affinity protein-metal interactions have not been frequently observed, although proteins that bind very effectively to metal surfaces have been documented.[63] The pilin receptor binding domain may represent a novel protein architecture that has evolved primarily for adherence to surfaces. It is interesting to note that other bacterial T4P have recently been observed to function as nano-wires to transfer electrons to, or from the bacterial cell surface and metals in the environment.[64, 65] The nature of the molecular interaction that occurs between the metal surface and the peptide remains somewhat enigmatic, and is complicated by the complexity of a real world metal surface.

4.3. PNT Steel Binding and Potential Applications

The melding of biochemically acceptable functionalities onto abiotic substrates such as CNTs[4–7] is exciting for the development of biologically amenable nanosystems. However, despite the unique physical and electrochemical properties of CNTs, current synthetic and purification strategies[66] hinder their acceptance in biological systems.[10, 11] To develop a more biologically accepted nanosystem, we have attempted to adapt an existing nanostructure present in the natural world.[17] The T4P from *P. aeruginosa* is an ideal template system from which to begin this process; these multi-functional nanostructures provide the bacterium a means of communication (with its environment and surrounding cells), motility, and adherence to a variety of biotic and abiotic surfaces.[20, 22, 36, 43–46]

The observation that *P. aeruginosa* T4P mediates adherence to stainless steel surfaces[20] prompted our investigation into the potential that pilin-derived PNTs may also mediate similar interactions. Indeed, PNTs were observed to bind stainless steel (Fig. 5). Surface binding by T4P is known to be a tip associated process,[43, 46] and current assembly models[34–36] present a limited number of accessible binding sites at the tip of the T4P. PNTs binding to stainless steel was readily inhibited by direct competition with a monovalent ligand, indicating that PNTs, like T4P, bind surfaces via a limited number of receptor binding domains displayed at their tips. If PNT binding was not tip-associated, a much larger, non-saturable binding of the steel surface by PNTs would be expected, based on the increased number of binding domains presented by the PNT quaternary structure, and a monovalent ligand would be unable to inhibit the binding of such a multivalent ligand.

The adherence of biochemical moieties to abiotic substrates is of considerable interest in a range of disciplines, including biology, biochemistry, surface and materials chemistry, and nanotechnology. Indeed, the presentation of distinct nucleic acid sequences on a surface is the basis of microarray technology, has revolutionized the analysis of genomes,[67] and has fostered considerable interest in the physicochemical properties of these

unique interfaces.[68, 69] Therefore, the adherence of PNTs to surfaces should lead to novel metallo-biomolecular interfaces, and applications. Our results suggest that a pre-fabrication of PNTs, "loaded" with additional ligands within the solvent accessible interior of the PNTs or coupled to the external surface of the PNTs, could be utilized to fabricate derivatized PNT tip-coupled D transition metal surfaces. These biometallic interfaces or surfaces could be used to generate sensor electrodes, electronically controlled pumps, or molecular scaffolds for various nanotech applications.

References and Notes

1. V. Georgakilas, K. Kordatos, M. Prato, D. M. Guldi, M. Holzinger, and A. Hirsch, *J. Am. Chem. Soc.* 124, 760 (**2002**).
2. V. Georgakilas, N. Tagmatarchis, D. Pantarotto, A. Bianco, J. P. Briand, and M. Prato, *Chem. Commun. (Camb)* 24, 3050 (**2002**).
3. H. W. C. Postma, T. Teepen, Z. Yao, M. Grifoni, and C. Dekker, *Science* 293, 76 (**2001**).
4. S. S. Wong, E. Joselevich, A. T. Woolley, C. L. Cheung, and C. M. Lieber, *Nature* 394, 52 (**1998**).
5. D. Pantarotto, C. D. Partidos, J. Hoebeke, F. Brown, E. Kramer, J. P. Briand, S. Muller, M. Prato, and A. Bianco, *Chem. Biol.* 10, 961 (**2003**).
6. V. Lovat, D. Pantarotto, L. Lagostena, B. Cacciari, M. Grandolfo, M. Righi, G. Spalluto, M. Prato, and L. Ballerini, *Nano Lett.* 5, 1107 (**2005**).
7. G. Korneva, H. Ye, Y. Gogotsi, D. Halverson, G. Friedman, J. C. Bradley, and K. G. Kornev, *Nano Lett.* 5, 879 (**2005**).
8. Z. Wu, Z. Chen, X. Du, J. M. Logan, J. Sippel, M. Nikolou, K. Kamaras, J. R. Reynolds, D. B. Tanner, A. F. Hebard, and A. G. Rinzler, *Science* 305, 1273 (**2004**).
9. N. W. Kam, Z. Liu, and H. Dai, *Angew. Chem. Int. Ed. Engl.* 45, 577 (**2006**).
10. G. Jia, H. Wang, L. Yan, X. Wang, R. Pai, T. Yan, Y. Zhao, and X. Guo, *Environ. Sci. Technol.* 39, 1378 (**2005**).
11. A. Margez, S. Kasas, V. Salicio, N. Pasquier, J. W. Seo, M. Celio, V. Catsicas, B. Schwaller, and L. Forro, *Nano Lett.* 6, 1121 (**2006**).
12. D. Cui, F. Tian, C. S. Ozkan, M. Wang, and H. Gao, *Toxicol. Lett.* 155, 73 (**2005**).
13. X. Chen, U. C. Tam, J. L. Czlapinski, G. S. Lee, D. Rabuka, A. Zettl, and C. R. Bertozzi, *J. Am. Chem. Soc.* 128, 6292 (**2006**).
14. G. Lu, T. Komatsu, and E. Tsuchida, *Chem. Commun.* 28, 2980 (**2007**).
15. S. Hou, J. Wang, and C. R. Martin, *Nano Lett.* 5, 231 (**2005**).
16. F. Patolsky, Y. Weizmann, and I. Willner, *Nat. Materials* 3, 692 (**2004**).
17. G. F. Audette, E. J. van Schaik, B. Hazes, and R. T. Irvin, *Nano Lett.* 4, 1897 (**2004**).
18. G. P. Bodey, R. Bolivar, V. Fainstein, and L. Jadeja, *Rev. Infect. Dis.* 5, 279 (**1983**).
19. D. E. Woods, D. C. Straus, W. G. Johanson, Jr., V. K. Berry, and J. A. Bass, *Infect. Immun.* 29, 1146 (**1980**).

20. C. L. Giltner, E. J. van Schaik, G. F. Audette, D. Kao, R. S. Hodges, D. J. Hassett, and R. T. Irvin, *Mol. Microbiol.* 59, 1083 (**2006**).

21. W. Folkhard, D. A. Marvin, T. H. Watts, and W. Paranchych, *J. Mol. Biol.* 149, 79 (**1981**).

22. G. F. Audette and B. Hazes, *J. Nanosci. Nanotechnol.* 7, 2222 (**2007**).

23. W. Paranchych, P. A. Sastry, L. S. Frost, M. Carpenter, G. D. Armstrong, and T. H. Watts, *Can. J. Microbiol.* 25, 1175 (**1979**).

24. G. F. Audette, R. T. Irvin, and B. Hazes, *Acta Crystallogr. D Biol. Crystallogr.* 59, 1665 (**2003**).

25. G. F. Audette, R. T. Irvin, and B. Hazes, *Biochemistry* 43, 11427 (**2004**).

26. A. Torii, M. Sasaki, K. Hane, and S. Okuma, *IEEE* 111 (**1993**).

27. W. R. Bowen, R. W. Lovitt, and C. J. Wright, *J. Colloid Interface Sci.* 228, 428 (**2003**).

28. H. Chao, M. E. Houston, Jr., S. Grothe, C. M. Kay, M. O'Connor-McCourt, R. T. Irvin, and R. S. Hodges, *Biochemistry* 35, 12175 (**1996**).

29. H. Chao, D. L. Bautista, J. Litowski, R. T. Irvin, and R. S. Hodges, *J. Chromatogr. B Biomed. Sci. Appl.* 715, 307 (**1998**).

30. B. Tripet, L. Yu, D. L. Bautista, W. Y. Wong, R. T. Irvin, and R. S. Hodges, *Protein Eng.* 9, 1029 (**1996**).

31. G. De Crescenzo, J. R. Litowski, R. S. Hodges, and M. O'Connor-McCourt, *Biochemistry* 42, 1754 (**2003**).

32. J. R. Litowski and R. S. Hodges, *J. Pept. Res.* 58, 477 (**2001**).

33. H. E. Parge, K. T. Forest, M. J. Hickey, D. A. Christensen, E. D. Getzoff, and J. A. Tainer, *Nature* 378, 32 (**1995**).

34. B. Hazes, P. A. Sastry, K. Hayakawa, R. J. Read, and R. T. Irvin, *J. Mol. Biol.* 299, 1005 (**2000**).

35. D. W. Keizer, C. M. Slupsky, M. Kalisiak, A. P. Campbell, M. P. Crump, P. A. Sastry, B. Hazes, R. T. Irvin, and B. D. Sykes, *J. Biol. Chem.* 276, 24186 (**2001**).

36. L. Craig, M. E. Pique, and J. A. Tainer, *Nat. Rev. Microbiol.* 2, 363 (**2004**).

37. H. S. Park, M. Wolfgang, J. P. van Putten, D. Dorward, S. F. Hayes, and M. Koomey, *Mol. Microbiol.* 42, 293 (**2001**).

38. L. Craig, N. Volkmann, A. S. Arvai, M. E. Pique, M. Yeager, E. H. Egelman, and J. A. Tainer, *Mol. Cell* 23, 651 (**2006**).

39. J. S. Mattick, *Annu. Rev. Microbiol.* 56, 289 (**2002**).

40. X. Nassif, J. L. Beretti, J. Lowy, P. Stenberg, P. O'Gaora, J. Pfeifer, S. Normark, and M. So, *Proc. Natl. Acad. Sci. U.S.A.* 91, 3769 (**1994**).

41. T. Rudel, I. Scheuerpflug, and T. F. Meyer, *Nature* 373, 357 (**1995**).

42. R. T. Irvin, P. Doig, K. K. Lee, P. A. Sastry, W. Paranchych, T. Todd, and R. S. Hodges, *Infect. Immun.* 57, 3720 (**1989**).

43. K. K. Lee, H. B. Sheth, W. Y. Wong, R. Sherburne, W. Paranchych, R. S. Hodges, C. A. Lingwood, H. Krivan, and R. T. Irvin, *Mol. Microbiol.* 11, 705 (**1994**).

44. H. Remaut and G. Waksman, *Curr. Opin. Struct. Biol.* 14, 161 (**2004**).

45. E. Van Haecke, J.-P. Remon, M. Moors, F. Raes, D. De Rudder, and A. van Peteghem, *Appl. Environ. Microb.* 56, 788 (**1990**).

46. R. T. Irvin, P. C. Doig, P. A. Sastry, B. Heller, and W. Paranchych, *Microbial. Ecol. Health Dis.* 3, 39 (**1989**).

47. G. Galli, *Proc. Natl. Acad. Sci. U.S.A.* 104, 2557 (**2007**).

48. B. Widom and D. Ben-Amotz, *Proc. Natl. Acad. Sci. U.S.A.* 103, 18887 (**2006**).

49. D. Y. Li and W. Li, *Appl. Phys. Lett.* 79, 4337 (**2001**).

50. W. Li and D. Y. Li, *Surf. Rev. Lett.* 11, 173 (**2004**).

51. W. Li and D. Y. Li, *Mater. Sci. Tech.* 18, 1057 (**2002**).

52. W. Li and D. Y. Li, *Appl. Surf. Sci.* 240, 388 (**2005**).

53. J. M. Skerker and H. C. Berg, *Proc. Natl. Acad. Sci. U.S.A.* 98, 6901 (**2001**).

54. A. Touhami, M. H. Jericho, J. M. Boyd, and T. J. Beveridge, *J. Bacteriol.* 188, 370 (**2006**).

55. C. E. Zobell, *Proc. Natl. Acad. Sci. U.S.A.* 21, 517 (**1935**).

56. C. E. Zobell, *J. Bacteriol.* 46, 39 (**1943**).

57. B. Li and B. E. Logan, *Colloids Surf. B Biointerfaces* 36, 81 (**2004**).

58. M. Morra and C. Cassinelli, *J. Biomater. Sci. Polym. Ed.* 9, 55 (**1997**).

59. C. I. Pereni, Q. Zhao, Y. Liu, and E. Abel, *Colloids Surf. B Biointerfaces* 48, 143 (**2006**).

60. J.-Y. Suh, L. Spyracopoulos, D. W. Keizer, R. T. Irvin, and B. D. Sykes, *Biochemistry* 40, 3985 (**2001**).

61. A. P. Campbell, L. Spyracopoulos, R. T. Irvin, and B. D. Sykes, *J. Biomol. NMR* 17, 239 (**2000**).

62. P. A. Campbell, W. Y. Wong, M. Houston, Jr., F. Schweizer, P. K. Cachia, R. T. Irvin, O. Hindsgaul, R. S. Hodges, and B. D. Sykes, *J. Mol. Biol.* 267, 382 (**1997**).

63. P. A. Suci and G. G. Geesey, *Colloids Surf. B Biointerfaces* 22, 159 (**2001**).

64. Y. A. Gorby, S. Yanina, J. S. McLean, K. M. Rosso, D. Moyles, A. Dohnalkova, T. J. Beveridge, I. S. Chang, B. H. Kim, K. S. Kim, D. E. Culley, S. B. Reed, M. F. Romine, D. A. Saffarini, E. A. Hill, L. Shi, D. A. Elias, D. W. Kennedy, G. Pinchuk, K. Watanabe, S. Ishii, B. Logan, K. H. Nealson, and J. K. Fredrickson, *Proc. Nat. Acad. Sci. U.S.A.* 103, 11358 (**2006**).

65. G. Reguera, K. P. Nevin, J. S. Nicoll, S. F. Covalla, T. L. Woodard, and D. R. Lovley, *Appl. Environ. Microbiol.* 72, 7345 (**2006**).

66. P. M. Ajayan, J. Charlier, and A. G. Rinzler, *Proc. Natl. Acad. Sci. U.S.A.* 96, 14199 (**1999**).

67. M. Chee, R. Yang, E. Hubbell, A. Berno, X. C. Huang, D. Stern, J. Winkler, D. J. Lockhart, M. S. Morris, and S. P. A. Fodor, *Science* 274, 610 (**1996**).

68. R. Levicky and A. Horgan, *TRENDS Biotechnol.* 23, 143 (**2005**).

69. G. Shen, N. Tercero, M. A. Gaspar, B. Varughese, K. Shepard, and R. Levicky, *J. Am. Chem. Soc.* 128, 8427 (**2006**).